



## ARTICLE

# PET imaging of kappa opioid receptors and receptor expression quantified in neuron-derived extracellular vesicles in socially housed female and male cynomolgus macaques

Bernard N. Johnson<sup>1,2</sup>, Ashish Kumar<sup>3</sup>, Yixin Su<sup>3</sup>, Sangeeta Singh<sup>3</sup>, Kiran Kumar Solingapuram Sai<sup>2,4</sup>, Susan H. Nader<sup>1</sup>, Songye Li<sup>5</sup>, Beth A. Reboussin<sup>6</sup>, Yiyun Huang<sup>5</sup>, Gagan Deep<sup>2,3,7</sup>✉ and Michael A. Nader<sup>1,2,4,7</sup>✉

© The Author(s), under exclusive licence to American College of Neuropsychopharmacology 2022

Recent positron emission tomography (PET) studies of kappa opioid receptors (KOR) in humans reported significant relationships between KOR availability and social status, as well as cocaine choice. In monkey models, social status influences physiology, receptor pharmacology and behavior; these variables have been associated vulnerability to cocaine abuse. The present study utilized PET imaging to examine KOR availability in socially housed, cocaine-naïve female and male monkeys, and peripheral measures of KORs with neuron-derived extracellular vesicles (NDE). KOR availability was assessed in dominant and subordinate female and male cynomolgus macaques ( $N = 4/\text{rank}/\text{sex}$ ), using PET imaging with the KOR selective agonist [ $^{11}\text{C}$ ]EKAP. In addition, NDE from the plasma of socially housed monkeys ( $N = 13/\text{sex}$ ;  $N = 6\text{--}7/\text{rank}$ ) were isolated by immunocapture method and analyzed for OPRK1 protein expression by ELISA. We found significant interactions between sex and social rank in KOR availability across 12 of 15 brain regions. This was driven by female data, in which KOR availability was significantly higher in subordinate monkeys compared with dominant monkeys; the opposite relationship was observed among males, but not statistically significant. No sex or rank differences were observed for NDE OPRK1 concentrations. In summary, the relationship between brain KOR availability and social rank was different in female and male monkeys. This was particularly true in female monkeys. We hypothesize that lower [ $^{11}\text{C}$ ]EKAP binding potentials were due to higher concentrations of circulating dynorphin, which is consistent with greater vulnerability in dominant compared with subordinate females. These findings suggest that the KOR is an important target for understanding the neurobiology associated with vulnerability to abused drugs and sex differences, and detectable in peripheral circulation.

*Neuropsychopharmacology* (2023) 48:410–417; <https://doi.org/10.1038/s41386-022-01444-9>

## INTRODUCTION

Drug abuse continues to be a major public health problem worldwide, resulting in deleterious consequences that affect health, social, and economic welfare [1]. In the United States, the societal cost of drug abuse is over \$820 billion, with approximately 20.3 million people over the age of 12 having met the DSM-V criteria for substance use disorder (SUD) in 2018 [2, 3]. SUD is a multifactorial disorder resulting from complex interactions between the pharmacological effects of a drug, biological characteristics of the individual, and environmental factors that render some individuals vulnerable [4]. As such, only a subset of individuals that use drugs of abuse develop SUDs. Similarly, individual differences in SUDs are observed in treatment efficacy and response to exogenous challenges (e.g., social stress, environmental enrichment) [5–7]. These variables are likely to contribute to the heterogeneity common in clinical studies, thus stressing the importance of a personalized

treatment approach for SUDs, similar to other CNS disorders [8]. The goal of the present study was to further evaluate a biological marker associated with vulnerability to cocaine use disorders (CUDs).

For these studies, the model of enrichment and chronic stress involves social housing of female and male cynomolgus macaques (e.g., [9, 10]). Macaques form a dominance hierarchy that is based on the outcomes of fights, with winners being considered dominant to losers. Evidence indicates that social status profoundly influences physiology. For example, the subordinate monkeys have been shown to be more susceptible to reproductive dysfunction [11], upper respiratory infection [12] and atherosclerosis [13]. Furthermore, the finding that subordinate monkeys had heavier adrenal glands compared to dominant monkeys [14], support the hypothesis that social status can differentially affect the physiology of the HPA axis [15]. On the other end of the continuum, we have hypothesized that

<sup>1</sup>Department of Physiology and Pharmacology, Wake Forest University School of Medicine, Winston-Salem, NC, USA. <sup>2</sup>Center for Addiction Research, Wake Forest University School of Medicine, Winston-Salem, NC, USA. <sup>3</sup>Department of Cancer Biology, Wake Forest University School of Medicine, Winston-Salem, NC, USA. <sup>4</sup>Department of Radiology, Wake Forest University School of Medicine, Winston-Salem, NC, USA. <sup>5</sup>Yale PET Center, Department of Radiology and Biomedical Imaging, Yale University School of Medicine, New Haven, CT, USA. <sup>6</sup>Department of Biostatistics and Data Sciences, Wake Forest University School of Medicine, Winston-Salem, NC, USA. <sup>7</sup>These authors jointly supervised this work: Gagan Deep, Michael A. Nader. ✉email: [gdeep@wakehealth.edu](mailto:gdeep@wakehealth.edu); [mnader@wakehealth.edu](mailto:mnader@wakehealth.edu)

Received: 13 May 2022 Revised: 27 July 2022 Accepted: 24 August 2022

Published online: 13 September 2022

becoming dominant in the social group represents conditions of environmental enrichment [16, 17].

Initial positron emission tomography (PET) research on cocaine abuse focused primarily on the dopamine (DA) receptor system, and in particular, the DA D2/D3 receptors (D2/D3R). In humans, almost exclusively men, individuals with a long-history of cocaine use had lower measures of D2/D3R availability compared with age-matched control subjects [18]. This finding was extended to nonhuman primates (NHPs) using a within-subjects design showing that cocaine self-administration (SA) resulted in dose-dependent decreases in D2/D3R availability in all monkeys [19]. As it relates to measures of vulnerability, Volkow et al. [20] noted that non-substance abusing men with lower measures of D2/D3R availability reported rewarding subjective responses to methylphenidate, suggesting an inverse relationship between D2/D3R availability and stimulant reinforcement. This finding was replicated in socially housed male monkeys, showing that dominant males had higher measures of D2/D3R than subordinate males, and were less vulnerable to cocaine SA [21]. Importantly, similar results have been observed in humans [22, 23]. However, in socially housed female monkeys, subordinate animals had lower D2/D3R availability, but were less sensitive to cocaine reinforcement compared with dominant female monkeys [24]. Thus, there appears to be sex differences in the role of D2/D3R availability and vulnerability to cocaine reinforcement.

While DA is associated with euphoria, an opposing neurobiological system, the kappa opioid receptor (KOR) system, and its endogenous ligand dynorphin, is an integral part of the brain's stress response system and is implicated in the neurobiological regulation of aversive states, including negative reinforcement associated with SUDs [25–29], sometimes referred to as the “dark side” of addiction, an allostatic dynamic of decreasing brain reward and recruitment of stress systems [26, 30–34]. This allostatic dynamic, negative affective state, can lead to the transition from social drug use to SUD [31–33]. Both chronic stress and cocaine exposure increase dynorphin/KOR system function, promoting dysregulation, negative affective states and stress reactivity [26, 27, 30, 35].

A recent PET study in humans investigated the relationship between KOR system and social status [36] utilizing a novel KOR agonist tracer [<sup>11</sup>C]EKAP [37, 38]. KOR availability inversely correlated with social status such that lower social status was associated with higher KOR availability in “anti-reward”/stress brain regions. Additionally, sex differences in KOR availability were observed, with females having higher KOR availability than males [36], consistent with clinical literature showing women have greater responses to KOR agonists than men [39–41]. A subsequent PET study in subjects with CUD (all males) reported a significant association between KOR availability and cocaine choice [42], implicating differences in KOR availability with cocaine choice and stress-induced relapse [42, 43]. These studies suggest KOR availability as a potential mechanism mediating sex differences in vulnerability to cocaine abuse. Thus, one goal of the present study was to extend the characterization of brain KOR availability, using [<sup>11</sup>C]EKAP, to socially housed female and male monkeys.

While PET imaging is an excellent in vivo measure of brain function, identifying potential peripheral markers of KOR function would provide greater clinical utility. Thus, a second goal was to identify and quantify protein expression levels of the KOR gene OPRK1 in neuron-derived extracellular vesicles (NDE), obtained from plasma of socially housed monkeys. Extracellular vesicles (EVs) are lipid-bound vesicles secreted by cells into the extracellular space and play a key role in intercellular communication and maintenance of cellular homeostasis. EVs have been reported in almost every bodily fluid and their cargo (e.g., proteins, RNAs, lipids, and metabolites, etc.) has been extensively characterized and correlated with normal or pathophysiological

states [44–48]. Moreover, in recent years NDE in plasma have shown promise as a potential biomarker for early diagnosis and therapeutic outcomes in various neurocognitive disorders [46, 47]. A recent study from our lab reported the usefulness of NDE in better understanding the pro-inflammatory and neurodegenerative consequence of oxycodone SA in male cynomolgus monkeys [45]. Moreover, the cargos (both proteins and miRNAs) of NDE are shown to be associated with adverse clinical neurodevelopmental outcomes [49]. The present study is the first to examine OPRK1 expression in NDE, which will serve as a peripheral measure of KOR function.

## METHODS AND MATERIALS

### Subjects

Experimentally naive female and male cynomolgus monkeys (*Macaca fascicularis*), living in same-sex, stable ( $\geq 18$  months) social groups of four, served as subjects (Table 1). Social hierarchy is linear, from the most dominant (#1-ranked) to the most subordinate (#4-ranked) monkey, and was determined according to the outcomes of agonistic encounters as described previously [50–52]. For PET studies,  $N = 8$ /sex (4 dominant and 4 subordinate/sex) and for OPRK1 expression studies,  $N = 13$ /sex (6 dominant and 7 subordinate/sex). Monkeys were naive to drugs except for infrequent exposure to ketamine (IM), used for veterinary or imaging procedures. Monkeys lived in stainless steel cages (Allentown Caging,

**Table 1.** Individual characteristics of cocaine-naïve subjects used in the NDE and PET imaging procedures.

	Rank	Age	Weight (kg)	EKAP PET
Female				
C-8535	1	13	5.6	Y
C-8537	1	12	4.6	Y
C-8555	1	4	2.5	Y
C-8551	1	4	2.8	N
C-8554	2	4	2.5	Y
C-8550	2	4	3.7	N
C-8540	3	12	4.0	Y
C-8549	3	4	3.1	Y
C-8553	3	4	2.3	N
C-8557	4	4	2.7	Y
C-8531	4	12	3.7	Y
C-8548	4	4	2.6	N
C-8552	4	4	2.6	N
Male				
C-8503	1	14	8.4	Y
C-8504	1	13	11.6	Y
C-8563	1	4	3.6	N
C-8502	2	14	8.3	Y
C-8505	2	13	9.5	Y
C-8560	2	4	3.2	N
C-8506	3	13	9.4	Y
C-8558	3	5	5.4	Y
C-8561	3	4	2.9	N
C-8507	4	14	8.5	Y
C-8559	4	5	3.9	Y
C-8562	4	5	3.7	N
C-8564	4	5	4.9	N

Y Subject used in the NDE and EKAP PET imaging procedures, N Subject used only in the NDE procedure.

Allentown, NJ) divided into four equal quadrants ( $0.71 \times 0.84 \times 0.84$  m) by removable wire mesh partitions. Partitions allowed visual, auditory and limited tactile interactions. When partitions were removed, four (same-sex) monkeys occupied the entire cage ( $0.71 \times 1.73 \times 1.83$  m). Each monkey was fitted with an aluminum collar (Primate Products, Redwood City, CA) and trained to sit in a standard primate chair (Primate Products). Monkeys were weighed weekly and fed enough food daily (Purina LabDiet 5045, St Louis, MO and fresh fruit and vegetables) to maintain a healthy body weight and appearance as determined by daily inspection and periodic veterinary examinations. Water was available *ad libitum* in the homecage. For female monkeys, menstrual cycle was monitored daily by vaginal swabs [53] and was approximately 28 days. The first indication of bleeding was indicative of menses and counted as day 1 of the cycle. We considered days 2–10 the follicular phase and days 19–28 the luteal phase of the menstrual cycle. All PET studies in females occurred in the follicular phase. All procedures were performed in accordance with the 2011 National Research Council Guidelines for the Care and Use of Mammals in Neuroscience and Behavioral Research and were approved by the Wake Forest University Animal Care and Use Committee.

### Experiment 1: Effects of sex and social rank on KOR availability

On separate days, socially housed female and male monkeys underwent a structural MRI and [ $^{11}\text{C}$ ]EKAP PET scans. All subjects received a 15 min structural MRI scan on a Siemens MAGNETOM Skyra 3-T scanner with TIM technology for image co-registration and assistance with the anatomic localization of regions of interest (ROI). Prior to the MRI scan, the monkey was anesthetized with ketamine (5.0 mg/kg, IM) and dexmedetomidine (0.04 mg/kg, IM) and then transported to the MRI Building. The reversal agent, atipamezole (0.4 mg/kg, IM) was administered following the scan. On the morning of the PET study, the monkey was anesthetized with ketamine (10 mg/kg, IM) and transported to the Wake Forest University School of Medicine PET Center. The monkey was intubated and anesthesia (isoflurane 1.5%) was maintained throughout the scan. A catheter was inserted into an external vein for tracer injection and fluid replacement throughout the study. Body temperature was maintained at 40°C and vital signs (e.g., heart rate, respiration rate,  $\text{O}_2$  saturation, etc.) were monitored throughout the scanning procedure. All PET studies were conducted with a GE 64 slice PET/CT Discover VCT scanner (GE Medical Systems, Milwaukee, WI). Before tracer administration, a 5 min transmission scan was acquired in three-dimensional mode. Next, [ $^{11}\text{C}$ ]EKAP ( $5 \pm 1$  mCi) was administered intravenously via manual injection, followed by a 120 min three-dimensional dynamic brain scan. At the end of the scan and following recovery from anesthesia/extubation, the monkey was returned to its homecage and remained singly housed for the day. The time between ketamine-induced anesthesia and the PET study was at least 60-min, thereby minimizing any pharmacological effects of ketamine on binding potential (BP). Two of the male monkeys were scanned twice, to obtain a measure of test-retest variability, which was ~3% (Table S1).

### PET imaging analysis and kinetic modeling

PET data were collected in list mode for 120 min and reformatted into 33 successive frames of increasing durations ( $6 \times 10$  s,  $3 \times 1$  min,  $2 \times 2$  min, and  $22 \times 5$  min). PET emission data were attenuation-corrected using the transmission scan, and dynamic images (33 frames and 256 slices over 120 min) were reconstructed using an automated QCHD8-based view point HD rebinning algorithm. PET images were co-registered to individual MRIs using PMOD Biomedical Image Quantification Software (version 3.1; PMOD Technologies, Zurich, Switzerland). Spherical ROIs, all 2.5 mm radii unless noted below, were drawn on individual MR images for the following brain regions: dorsal prefrontal cortex (dPFC), medial prefrontal cortex (mPFC), orbitofrontal cortex (OFC), anterior cingulate cortex (ACC), caudate nucleus, putamen, ventral striatum (2.0 mm radii), amygdala, globus pallidus, ventral claustrum (1.0 mm radii), insula (2.0 mm radii), cingulate cortex, hippocampus, thalamus (3.0 mm radii), temporal cortex and cerebellum (4.0 mm radii), which served as the reference region. Previous studies with KOR radiotracers, including [ $^{11}\text{C}$ ]EKAP, indicated that cerebellum can be used as a reference region in nonhuman primates to calculate BP [37, 54]. The primary dependent variable is the ratio of the distribution of radioligand in the region of interest to the distribution in the reference region. The distribution volume ratio can be converted to BP, which is a unitless number representing the ratio of receptor density to affinity ( $B_{\text{max}}/K_d$ ). For these studies, the BP was calculated for each ROI using the Simplified Reference Tissue model [55], which allowed for the generation

of binding parameters without obtaining arterial blood samples [37]. BPs for each region were not different between left and right sides and therefore data from each monkey were expressed as a mean of both sides.

### Experiment 2: Peripheral measures of KOR using NDEs

All blood samples were obtained from the femoral vein of awake monkeys, while seated in a primate restraint chair. First, total EVs (TE) were isolated from the plasma of monkeys using the ExoQuick (System Biosciences, Palo Alto California, USA) precipitation method as described by us previously [56, 57]. Next, NDE were pulled out from TE using two surface biomarkers (L1CAM/CD171 and synaptophysin) as previously described [45]. Briefly, we first used L1CAM positive NDE from TE using L1CAM/CD171-Biotin antibody (Cat. No. 13-1719-82, ThermoFisher Scientific) and streptavidin-tagged agarose beads (ThermoFisher Scientific, Waltham, MA, USA). To further purify NDE using the second marker, synaptophysin-biotin antibody and streptavidin-tagged agarose beads were used and double positive (both L1CAM and synaptophysin) NDE were collected. TE and/or NDE were characterized by nanoparticle tracking analyses (NTA), immunogold labeling and transmission electron microscopy, Exo-check antibody array and ELISA assays (methodology described in Supplementary Methods) following our published methods [45, 56].

### Data analyses

Two-way ANOVA was used to compare (1) PET measures of [ $^{11}\text{C}$ ]EKAP BP for each ROI (Experiment 1), and (2) NDE measure of OPRK1 expression by sex and social rank (Experiment 2). For these analyses, social rank was binary, with #1- and #2-ranked monkeys being “dominant” and #3- and #4-ranked monkeys being “subordinate”. An interaction was tested using a *t*-test. A post-hoc *F*-test with Bonferroni-Holm adjustment was used to determine social rank differences by sex. Normality assumptions were examined using the Shapiro-Wilk normality test. All data are presented as means and 95% confidence intervals. Spearman’s rank correlations were calculated between [ $^{11}\text{C}$ ]EKAP BP and social rank for each ROI and stratified by sex. Social rank was defined as an ordinal variable with values 1–4. Significance for all models was set at  $p < 0.05$ . For PET and NDE assessments, investigators were blind to the sex and social rank of the monkeys.

## RESULTS

### Experiment 1: Effects of sex and social rank on KOR availability

The regional binding potentials (mean  $\pm$  SD) of dominant and subordinate males and females for each of 15 ROIs, and the cerebellum, are shown in Table 2. A representative tissue-time activity curve is shown in Fig. S1. The normal distribution of the data was confirmed with the Shapiro-Wilk test for all ROIs, with the exception of the dPFC and the hippocampus. Log-transformations of these ROI did not impact findings; therefore, results are presented on the original scale. Two-way ANOVA indicated significant interactions between sex and social rank in the dPFC, ACC, caudate nucleus, putamen, ventral striatum, amygdala, globus pallidus, insula, claustrum, cingulate cortex, hippocampus and the temporal cortex (Table 2<sup>a</sup>). Three ROIs did not show an interaction between sex and social rank, though differential main effects were significant in these regions. The main effect of social rank on [ $^{11}\text{C}$ ]EKAP BP was significant in the mPFC [ $t_{(1,12)} = 2.53$ ,  $p < 0.05$ ] and the OFC [ $t_{(1,12)} = 2.55$ ,  $p < 0.05$ ], such that subordinates had higher BPs than their dominant counterparts. There was a significant main effect of sex on KOR BP in the thalamus [ $t_{(1,12)} = 2.88$ ,  $p < 0.05$ ], such that males had higher BP than females, but no social rank differences. There was no significant main effect of sex in the mPFC or OFC.

Post-hoc tests (Table 2<sup>b</sup>) indicated no significant differences in KOR BP between dominant and subordinate males. However, subordinate females had significantly higher KOR BP than dominant females in the dPFC, ACC, caudate nucleus, putamen, ventral striatum, amygdala, globus pallidus, insula, claustrum, cingulate cortex, hippocampus, and the temporal cortex. Representative images of dominant (#1) and subordinate (#4), male and female monkeys are shown in Fig. 1.

**Table 2.** [<sup>11</sup>C]EKAP BP across all ROIs in cocaine-naïve socially housed female and male monkeys (N = 8/sex).

ROI	Females				Males				Interaction		
	Dominant		Subordinate		Dominant		Subordinate		post-hoc <sup>b</sup>	Sex and Social Rank	
	Mean (SD)	Pr > F	F	post-hoc <sup>b</sup>	Mean (SD)	Pr > F	t-Value <sup>a</sup>	Pr >  t  <sup>a</sup>			
Dorsal PFC	0.46 (0.25)	0.01	13.9	0.01	0.68 (0.05)	0.93	0.01	0.01	0.93	-2.70	0.02
Medial PFC	0.77 (0.22)	0.052	6.42	0.052	0.84 (0.06)	0.91	0.01	0.01	0.91	-1.71	0.11
Orbito FC	0.75 (0.28)	0.051	6.51	0.051	1.03 (0.13)	0.47	0.56	0.56	0.47	-1.27	0.23
Anterior Cing Cortex	0.85 (0.20)	0.003	17.4	0.003	1.19 (0.14)	0.38	0.82	0.82	0.38	-2.31	0.04
Caudate	0.82 (0.21)	0.01	10.7	0.01	1.24 (0.18)	0.32	1.08	1.08	0.32	-3.05	0.01
Putamen	0.94 (0.15)	0.003	17.2	0.003	1.30 (0.11)	0.36	0.93	0.93	0.36	-3.61	0.004
Ventral Striatum	0.83 (0.07)	0.003	17.2	0.003	1.12 (0.02)	0.16	2.26	2.26	0.16	-4.00	0.002
Amygdala	0.84 (0.12)	0.04	7.54	0.04	1.02 (0.22)	0.31	1.13	1.13	0.31	-2.70	0.02
Globus Pallidus	0.78 (0.06)	0.01	10.8	0.01	1.01 (0.10)	0.07	3.87	3.87	0.07	-3.72	0.003
Insula	0.92 (0.15)	0.0005	26.5	0.0005	1.26 (0.10)	0.12	2.79	2.79	0.12	-4.82	0.0004
Clastrum	1.03 (0.14)	0.002	19.4	0.002	1.41 (0.12)	0.41	0.74	0.74	0.41	-3.72	0.003
Cingulate Cortex	0.73 (0.14)	0.0002	33.9	0.0002	1.19 (0.18)	0.78	0.08	0.08	0.78	-4.32	0.001
Hippocampus	0.79 (0.10)	0.03	7.86	0.03	0.77 (0.12)	0.15	2.35	2.35	0.15	-3.07	0.01
Thalamus	0.67 (0.30)	0.29	1.54	0.29	0.89 (0.20)	0.29	2.41	2.41	0.29	-1.98	0.07
Temporal Cortex	0.39 (0.04)	0.04	6.95	0.04	0.70 (0.21)	0.15	2.38	2.38	0.15	-2.95	0.01
Cerebellum	0.03 (0.02)	—	—	—	0.04 (0.06)	—	—	—	—	—	—

<sup>a</sup>Two-way ANOVA was used to compare [<sup>11</sup>C]EKAP BP for each ROI by sex and social rank.

<sup>b</sup>Post-hoc F-test with Bonferroni-Holm adjustment was used to determine social rank differences by sex. Bold values represent statistical significance.

In addition, Spearman's rank correlations were estimated within each sex, to determine the relationship between social rank on an ordinal scale (1,2,3,4) and KOR BPs. There was a strong, negative correlation between social rank and BPs in females ( $r_s(6) = -0.85$ ,  $p = 0.01$ ), confirming that dominant females had lower BPs compared with subordinate females. In contrast, there was a significant positive correlation in males ( $r_s(6) = 0.74$ ,  $p = 0.046$ ), confirming the opposite was true, with dominant males having higher BPs compared with subordinate males.

**Experiment 2: Characterization of TE, NDE, and identification of OPRK1**

Characterization of TE using NTA from both dominant and subordinate male and female monkeys did not show any significant difference in concentration, average size, protein concentration and distribution of size (Supplementary Results; Fig. S2A–B). Still, the size of the TE was <150 nm, which corresponds to a size range of small extracellular vesicles (sEVs). Typical sEVs/ exosomes markers were confirmed on isolated sEVs from plasma using antibody arrays (Fig. S2C). Moreover, characterization of NDE with immunogold labeling and transmission electron microscopy showed the presence of L1CAM and synaptophysin (markers used for NDE isolation) on NDE surface (Fig. S2D). Exo-check antibodies array for neuron- and exosome-specific markers confirmed the specificity and purity of the isolated NDE (Fig. S2E). Importantly, OPRK1 was quantified in NDE isolated from plasma in all animals (Fig. 2). Two-way ANOVA revealed there was no interaction [ $F_{(1,21)} = 2.03$ ,  $p = 0.16$ ] of sex and social rank on NDE OPRK1 concentrations. Furthermore, there were no differences in NDE OPRK1 concentrations between dominant and subordinate females [ $F_{(1,12)} = 0.06$ ,  $p > 0.05$ ], however, the trend is for OPRK1 concentrations to be higher for dominant males compared to subordinate males [ $F_{(1,11)} = 3.66$ ,  $p = 0.084$ ] (Fig. 2).

**DISCUSSION**

The goals of the present study were to examine the relationship between social rank and brain KOR availability in drug-naïve female and male monkeys and to assess the role of NDE OPRK1 expression as a peripheral biomarker of KOR availability. The main findings of this study were: (1) significant interaction between sex and social rank in [<sup>11</sup>C]EKAP BP in 12/15 brain regions; (2) [<sup>11</sup>C]EKAP BP correlated positively with social rank in males and negatively in females. Furthermore, the overall lowest receptor availability across ROIs was observed in dominant females and subordinate males, the two most vulnerable phenotypes to cocaine reinforcement [21, 24]; and (3) peripheral measures of KORs were identified and quantified by OPRK1 expression in NDE, with concentrations trending higher in dominant males compared with their subordinate counterpart, while no rank differences were observed in females.

Previous PET imaging studies from our laboratory focused on the role of DA D2/D3R availability in socially housed male and female monkeys. Consistent with other studies in male subjects, we noted that dominant male monkeys had higher levels of D2/D3R availability compared with subordinates and the latter were more vulnerable to cocaine reinforcement [21]. However, while D2/D3R availability was also higher in dominant females compared with subordinate females, it was the dominant females that were more vulnerable to cocaine reinforcement [24]. Thus, the present study aimed to extend the characterization of social status and sex to include another neurotransmitter system, the KOR, which appears to operate in opposition to the DA system [26, 27]. The current findings in males are analogous to D2/D3R availability, where [<sup>11</sup>C]EKAP BP is higher in dominant males compared with subordinate males. However, in females, the current findings are opposite to D2/D3R availability, where [<sup>11</sup>C]

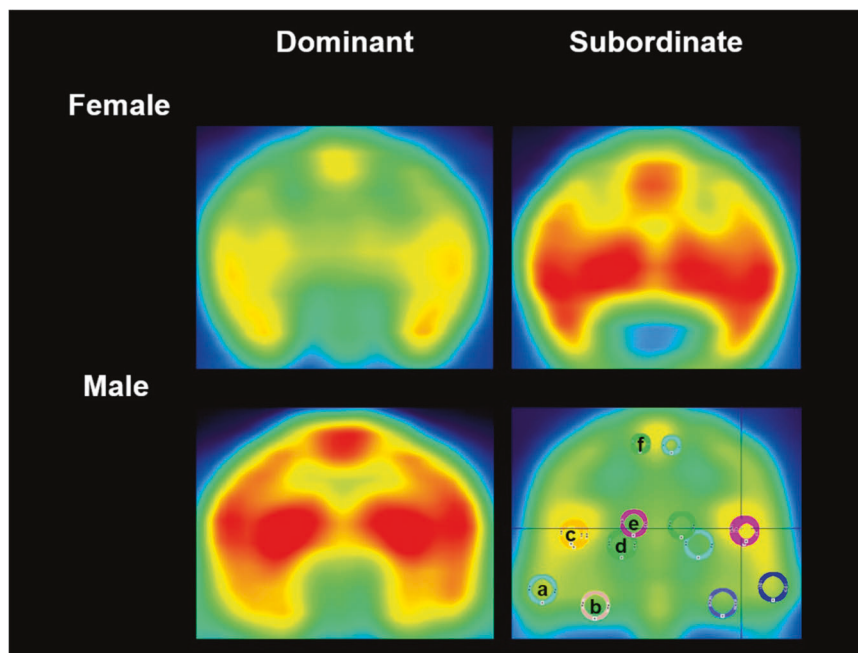


**Fig. 1** Representative PET/CT brain images with the KOR selective agonist [ $^{11}\text{C}$ ]EKAP in dominant (left) and subordinate (right), female (top) and male (bottom) cynomolgus monkeys. Subordinate females and dominant males have the higher KOR availability compared with dominant females and subordinate males (see also Table 2). Illustrated images are of slice 134, frame 17. The lower right image includes co-registered regions of interest labeled a–f. **a** Temporal cortex. **b** Hippocampus. **c** Insula and claustrum. **d** Globus pallidus. **e** Thalamus. **f** Cingulate cortex.

EKAP BP is significantly higher in subordinate compared with dominant females. Of note, the overall lowest BPs across ROI were observed in dominant females and subordinate males; these are the two most vulnerable phenotypes to cocaine reinforcement.

The highest KOR available were observed in subordinate females, with the four highest regions being the claustrum > insula > ACC > putamen. In dominant male monkeys, the claustrum and insula were also the regions with the highest KOR availability, followed by the putamen and caudate nucleus. The claustrum is believed to play a key role in decision-making [58], so higher KOR availability, perhaps indicative of lower dynorphin concentrations, in less vulnerable phenotypes is consistent with proposed relationships between vulnerability and decision making [59, 60]. Similarly, the higher KOR availability measures in brain regions associated with reinforcement, the caudate nucleus and putamen, are consistent with lower stress response and less vulnerable phenotypes. It remains to be determined whether these sex x social rank differences reflect stress-related effects. Previous studies from socially housed female and male monkeys have not reported significant differences in cortisol concentrations [51, 53, 61]. As described below, we believe the reasons for these sex and social rank differences are due to a combination of rank-related changes in KOR densities and the influence of circulating dynorphin.

While human PET studies showed no differences between people with CUD vs. controls, high-dose cocaine self-administration displaced the PET KOR tracer in humans, suggesting cocaine-induced elevations in dynorphin [42]. Taken together, the PET and receptor autoradiography data point to a critical role for dynorphin (in autoradiography, it is washed away and for PET, it is competing with the radiotracer which will influence the binding potentials). If dynorphin is important in the PET signal, then studying cocaine-naïve subjects and using BP as a predictor of vulnerability may be the most appropriate phase in the addiction cycle to study KORs. Future studies will be required to better address this. In addition, it should be noted that KOR system has been implicated in several psychiatric diseases,

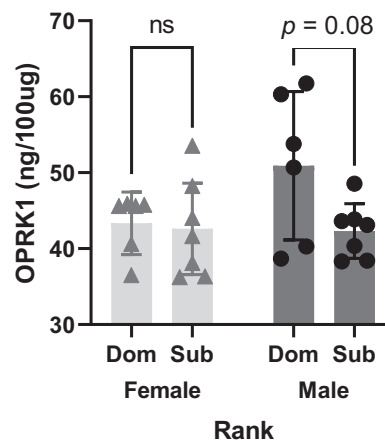


**Fig. 2** Relationship between social rank and NDE OPRK1 concentration in dominant (Dom) and subordinate (Sub) female (left) and male (right) cynomolgus monkeys ( $N = 13/\text{sex}$ ). OPRK1 expression in NDE was analyzed by ELISA and presented as ng/ml per 100 ug of NDE. Each bar represents mean and 95% confidence intervals for 26 monkeys ( $N = 13/\text{sex}$ ).

including depression, bipolar disorder, post-traumatic stress disorder, and schizophrenia [27, 62–64], therefore the study of [ $^{11}\text{C}$ ]EKAP in socially housed female and male monkeys may have implications for other diseases.

The highest [ $^{11}\text{C}$ ]EKAP BP in the claustrum is consistent with earlier autoradiography studies measuring KOR receptor densities in human and NHP brains [65, 66]. When stratified for sex and social rank, [ $^{11}\text{C}$ ]EKAP BP was: Sub Female > Dom Male > Sub Male > Dom Female. The claustrum has extensive connectivity with the neocortex, reciprocally connected with almost all cortical areas (most densely with medial regions of frontal cortex) and receives input from subcortical regions [67–70]. The broad and unique connections of the claustrum suggest it might serve as a

central network hub, and may play a fundamental role in a range of functions, associating sensory and limbic information to prompt attention by means of the frontal cortex and executive function control systems [68, 71, 72]. The proposed functional implications of claustrum connectivity with limbic–sensory–motor information could allow one to recognize a stimulus’ contextual importance and coordinate across the cortex to be able to direct focus to the most relevant stimuli [68, 72].

The second highest [ $^{11}\text{C}$ ]EKAP BP was observed in the insula, which is a structure involved in feelings of anxiety, pain, cognition, mood, threat recognition and conscious desires [73–77]. The insula is heavily involved in “interoception”, the integration of internal and external (environmental) stimuli, conveying it to the ACC, ventral striatum, mPFC to initiate adaptive responses, to guide behavior for the purposes of maintaining homeostasis [78–80]. Accordingly, the insula plays a major role in all aspects of decision making [77, 81]. The relevance of the insula to addiction first emerged with a study that showed that smokers with damage to the insula were able to quit smoking immediately and without cravings or relapse [82]. Other lesion studies have emerged, indicating that loss of activity in the insula best predicts smoking cessation with five-fold greater probability of quitting smoking [83, 84], experiencing less urges to smoke, along with less frequent and severe withdrawal symptoms [85, 86]. Imaging studies have further supported the relevance of the insula in addiction, showing differential insular activation during craving across multiple drug classes [87–89]. Of clinical significance, insular activity has been proposed to represent a potential biomarker for relapse risk and, as such, a target for transcranial magnetic stimulation (TMS) as a potential treatment for SUD [77, 80, 90–93].

Sex differences in KOR availability have been reported using PET imaging in humans. Using the KOR antagonist radiotracer [ $^{11}\text{C}$ ]LY2795050, males had higher KOR availability than females across most brain regions [94]. In contrast, using the KOR agonist radiotracer [ $^{11}\text{C}$ ]EKAP, Matuskey et al. [36], reported that females had significantly greater KOR availability than males. These differences may be attributed to the use of a KOR agonist vs. KOR antagonist PET tracer. Agonists bind with high affinity and interact with only the active state of the receptor, whereas antagonists bind with equal affinity to both the active and inactive states [37]. This discrepancy suggests females may have an augmented proportion of receptors in the active state in comparison to males. Interestingly, there is clinical literature to support this discrepancy, with women showing stronger clinical responses to KOR agonists than men [39–41].

PET imaging represents a highly translational research tool to investigate brain function in disease states. However, with that said, the ability to identify peripheral correlates associated with KOR function, would provide a rapid and inexpensive biomarker that clinicians may use to determine treatment strategies. As a result, we evaluated the use of NDE as peripheral biomarkers for KOR availability. Our two-round approach to isolate NDE from TE is highly novel - first we used a generic neuronal marker (L1CAM/CD171) and then a CNS neuron-specific marker (synaptophysin), yielding highly pure double positive NDE population. The present study was also the first to identify KOR signals in NDE, as measured by OPRK1 expression. Recently, we reported that expression of neurodegenerative biomarkers (NFL and  $\alpha$ -synuclein) correlated with differences in brain lobe volumes, using MRI analyses, between drug-naïve monkeys and those with an extended history of oxycodone SA [45]. In the present study, NDE OPRK1 expression trended towards significance in dominant male monkeys compared with subordinate males (see Fig. 2); the non-significant effect may be a result of a small sample size ( $N = 6\text{--}7/\text{rank}$ ). However, the trend showing higher expression in dominant males is consistent with the higher KOR BPs in dominant males, suggesting that OPRK1 expression is indicative of CNS KOR availability. The fact that there were no differences in

OPRK1 expression and social rank in females, while there were significant differences in KOR BP with [ $^{11}\text{C}$ ]EKAP, could indicate that the latter measures were, in fact, primarily influenced by circulating dynorphin, which would be consistent with greater vulnerability in dominant females. In the future, possible isolation of various brain-region specific NDE promises less invasive and more accurate measures of KORs in plasma.

There were some limitations to this study. For the PET imaging studies using a KOR agonist radiotracer, additional studies are needed to understand the mechanism(s) accounting for differences in BP between sexes and social groups. The human PET studies recently reported by Martinez et al. [42] utilized a KOR selective agonist [ $^{11}\text{C}$ ]GR103545 to investigate changes in the KOR/dynorphin system in subjects with CUD, before and after a cocaine binge. Following a 3-day cocaine binge, [ $^{11}\text{C}$ ]GR103545 binding showed a decrease in [ $^{11}\text{C}$ ]GR103545  $V_T$  of 14.4% across all brain regions. Martinez et al. [42] interpreted these decreases as representing increases in endogenous dynorphin concentrations. While multiple lines of evidence (rodent, NHP, human post-mortem) support binge cocaine greatly increasing dynorphin levels, the mechanism behind the decreases in [ $^{11}\text{C}$ ]GR103545 BP has not been identified and may involve receptor shift to inactive state, internalization or downregulation of the KOR, or a combination of these mechanisms [95]. A second limitation is conceptual: receptor binding studies of cocaine overdose victims indicate higher KOR densities [95] and elevated dynorphin concentrations [96] compared with controls, but we are speculating that lower KOR densities and higher dynorphin concentrations account for greater vulnerability. A particular advantage of using NHPs is that we can conduct longitudinal PET studies of how cocaine self-administration affects KOR availability, as well as study KOR agonists and antagonists on [ $^{11}\text{C}$ ]EKAP BP and behavior, to better address these potential discrepancies [25, 97–101]. Finally, there is the possibility that anesthetizing the monkeys with ketamine affected dynorphin concentrations, which could impact BP. We believe this is unlikely because of the 10–15 min half-life of IM ketamine [102] and the PET scan was not initiated for at least 60 min after ketamine-induced anesthesia.

## REFERENCES

1. UNODC, *Treatment of Stimulant Use Disorders: Current Practices and Promising Perspectives*, U.N.O.o.D.a. Crime, Editor. 2019.
2. SAMHSA, *Key substance use and mental health indicators in the United States: Results from the 2018 National Survey on Drug Use and Health*. (HHS Publication No. PEP19-5068, NSDUH Series H-54). Rockville, MD: Center for Behavioral Health Statistics and Quality, Substance Abuse and Mental Health Services Administration, 2019.
3. Buddy T. *How Drug Use Affects Our Society*. 2019.
4. Nader MA. Animal models for addiction medicine: From vulnerable phenotypes to addicted individuals. *Prog Brain Res*. 2016;224:3–24.
5. George O, Koob GF. Individual differences in the neuropsychopathology of addiction. *Dialogues Clin Neurosci*. 2017;19:217–29.
6. Koob GF, Volkow ND. Neurobiology of addiction: A neurocircuitry analysis. *Lancet Psychiatry*. 2016;3:760–73.
7. Johnson BN, NC, Minkiewicz M, Nader MA. Behavioral studies in nonhuman primates: Focus on models of substance use disorders, in *Encyclopedia of Behavioural Neuroscience*, S Della Sala, Editor. 2021, Elsevier. 1–12.
8. van der Stel J. Precision in addiction care: Does it make a difference? *Yale J Biol Med*. 2015;88:415–22.
9. Kaplan JR, Manuck SB, Clarkson TB, Lusso FM, Taub DM. Social status, environment, and atherosclerosis in cynomolgus monkeys. *Arteriosclerosis*. 1982;2:359–68.
10. Kaplan JR, Manuck SB, Adams MR, Weingand KW, Clarkson TB. Inhibition of coronary atherosclerosis by propranolol in behaviorally predisposed monkeys fed an atherogenic diet. *Circulation*. 1987;76:1364–72.
11. Cameron JL. Stress and behaviorally induced reproductive dysfunction in primates. *Semin Reprod Endocrinol*. 1997;15:37–45.
12. Cohen S, Line S, Manuck SB, Rabin BS, Heise ER, Kaplan JR. Chronic social stress, social status, and susceptibility to upper respiratory infections in nonhuman primates. *Psychosom Med*. 1997;59:213–21.

13. Kaplan JR, Manuck SB. Status, stress, and atherosclerosis: The role of environment and individual behavior. *Ann N. Y Acad Sci.* 1999;896:145–61.
14. Shively C, Kaplan J. Effects of social factors on adrenal weight and related physiology of *Macaca fascicularis*. *Physiol Behav.* 1984;33:777–82.
15. Henry JP, PM Stephens. *Stress, Health, and the Social Environment*. Topics in Environmental Physiology and Medicine. 1977: Springer New York, NY.
16. Nader MA, Czoty PW. PET imaging of dopamine D2 receptors in monkey models of cocaine abuse: genetic predisposition versus environmental modulation. *Am J Psychiatry.* 2005;162:1473–82.
17. Gould RW, Czoty PW, Porrino LJ, Nader MA. Social status in monkeys: Effects of social confrontation on brain function and cocaine self-administration. *Neuropsychopharmacology* 2017;42:1093–102.
18. Volkow ND, Fowler JS, Wolf AP, Schlyer D, Shiue CY, Alpert R, et al. Effects of chronic cocaine abuse on postsynaptic dopamine receptors. *Am J Psychiatry.* 1990;147:719–24.
19. Nader MA, Morgan D, Gage HD, Nader SH, Calhoun TL, Buchheimer N, et al. PET imaging of dopamine D2 receptors during chronic cocaine self-administration in monkeys. *Nat Neurosci.* 2006;9:1050–6.
20. Volkow ND, Wang GJ, Fowler JS, Logan J, Gatley SJ, Gifford A, et al. Prediction of reinforcing responses to psychostimulants in humans by brain dopamine D2 receptor levels. *Am J Psychiatry.* 1999;156:1440–3.
21. Morgan D, Grant KA, Gage HD, Mach RH, Kaplan JR, Prioleau O, et al. Social dominance in monkeys: Dopamine D2 receptors and cocaine self-administration. *Nat Neurosci.* 2002;5:169–74.
22. Martinez D, Orłowska D, Narendran R, Slifstein M, Liu F, Kumar D, et al. Dopamine type 2/3 receptor availability in the striatum and social status in human volunteers. *Biol Psychiatry.* 2010;67:275–8.
23. Martinez D, Carpenter KM, Liu F, Slifstein M, Broft A, Friedman AC, et al. Imaging dopamine transmission in cocaine dependence: link between neurochemistry and response to treatment. *Am J Psychiatry.* 2011;168:634–41.
24. Nader MA, Nader SH, Czoty PW, Riddick NV, Gage HD, Gould RW, et al. Social dominance in female monkeys: Dopamine receptor function and cocaine reinforcement. *Biol Psychiatry.* 2012;72:414–21.
25. Banks ML. The rise and fall of Kappa-opioid receptors in drug abuse research. *Handb Exp Pharmacol.* 2019;258:147–65.
26. Karkhanis A, Holleran KM, Jones SR. Dynorphin/Kappa Opioid Receptor Signaling in Preclinical Models of Alcohol, Drug, and Food Addiction. *Int Rev Neurobiol.* 2017;136:53–88.
27. Tejada HA, Bonci A. Dynorphin/kappa-opioid receptor control of dopamine dynamics: Implications for negative affective states and psychiatric disorders. *Brain Res.* 2019;1713:91–101.
28. Carlezon WA Jr, Krystal AD. Kappa-opioid antagonists for psychiatric disorders: From bench to clinical trials. *Depress Anxiety.* 2016;33:895–906.
29. Helal MA, Habib ES, Chittiboyina AG. Selective kappa opioid antagonists for treatment of addiction, are we there yet? *Eur J Med Chem.* 2017;141:632–47.
30. Trifilieff P, Martinez D. Kappa-opioid receptor signaling in the striatum as a potential modulator of dopamine transmission in cocaine dependence. *Front Psychiatry.* 2013;4:44.
31. Wemm SE, Sinha R. Drug-induced stress responses and addiction risk and relapse. *Neurobiol Stress.* 2019;10:100148.
32. Koob GF, Schulkin J. Addiction and stress: An allostatic view. *Neurosci Biobehav Rev.* 2019;106:245–62.
33. Wee S, Koob GF. The role of the dynorphin-kappa opioid system in the reinforcing effects of drugs of abuse. *Psychopharmacology.* 2010;210:121–35.
34. Hogarth L. Addiction is driven by excessive goal-directed drug choice under negative affect: Translational critique of habit and compulsion theory. *Neuropsychopharmacology.* 2020;45:720–35.
35. Ironside M, Kumar P, Kang MS, Pizzagalli DA. Brain mechanisms mediating effects of stress on reward sensitivity. *Curr Opin. Behav Sci.* 2018;22:106–13.
36. Matuskey D, Dias M, Naganawa M, Pittman B, Henry S, Li S, et al. Social status and demographic effects of the kappa opioid receptor: A PET imaging study with a novel agonist radiotracer in healthy volunteers. *Neuropsychopharmacology.* 2019;44:1714–9.
37. Li S, Zheng MQ, Naganawa M, Kim S, Gao H, Kapinos M, et al. Development and in vivo evaluation of a kappa-Opioid Receptor Agonist as a PET radiotracer with superior imaging characteristics. *J Nucl Med.* 2019;60:1023–30.
38. Naganawa M, Li S, Nabulsi N, Lin SF, Labaree D, Ropchan J, et al. Kinetic Modeling and Test-Retest Reproducibility of (11)C-EKAP and (11)C-FEKAP, Novel Agonist Radiotracers for PET Imaging of the kappa-Opioid Receptor in Humans. *J Nucl Med.* 2020;61:1636–42.
39. Gear RW, Gordon NC, Heller PH, Paul S, Miaskowski C, Levine JD. Gender difference in analgesic response to the kappa-opioid pentazocine. *Neurosci Lett.* 1996;205:207–9.
40. Gear RW, Miaskowski C, Gordon NC, Paul SM, Heller PH, Levine JD. Kappa-opioids produce significantly greater analgesia in women than in men. *Nat Med.* 1996;2:1248–50.
41. Gear RW, Miaskowski C, Gordon NC, Paul SM, Heller PH, Levine JD. The kappa opioid nalbuphine produces gender- and dose-dependent analgesia and anti-analgesia in patients with postoperative pain. *Pain* 1999;83:339–45.
42. Martinez D, Slifstein M, Matuskey D, Nabulsi N, Zheng MQ, Lin SF, et al. Kappa-opioid receptors, dynorphin, and cocaine addiction: A positron emission tomography study. *Neuropsychopharmacology* 2019;44:1720–7.
43. Blevins D, Martinez D. Role for kappa-opioid system in stress-induced cocaine use uncovered with PET. *Neuropsychopharmacology* 2020;45:233–4.
44. Fiandaca MS, Kapogiannis D, Mapstone M, Boxer A, Eitan E, Schwartz JB, et al. Identification of preclinical Alzheimer's disease by a profile of pathogenic proteins in neurally derived blood exosomes: A case-control study. *Alzheimers Dement.* 2015;11:600–7.e1
45. Kumar A, Kim S, Su Y, Sharma M, Kumar P, Singh S, et al. Brain cell-derived exosomes in plasma serve as neurodegeneration biomarkers in male cynomolgus monkeys self-administering oxycodone. *EBioMedicine.* 2021;63:103192.
46. Saeedi S, et al. Neuron-derived extracellular vesicles enriched from plasma show altered size and miRNA cargo as a function of antidepressant drug response. *Mol Psychiatry* 2021;26:7417–24.
47. Pulliam L, Sun B, Mustapic M, Chawla S, Kapogiannis D. Plasma neuronal exosomes serve as biomarkers of cognitive impairment in HIV infection and Alzheimer's disease. *J Neurovirol.* 2019;25:702–9.
48. Winston CN, Goetzl EJ, Akers JC, Carter BS, Rockenstein EM, Galasko D, et al. Prediction of conversion from mild cognitive impairment to dementia with neuronally derived blood exosome protein profile. *Alzheimers Dement (Amst).* 2016;3:63–72.
49. Goetzl L, Thompson-Felix T, Darbinian N, Merabova N, Merali S, Merali C, et al. Novel biomarkers to assess in utero effects of maternal opioid use: First steps toward understanding short- and long-term neurodevelopmental sequelae. *Genes Brain Behav.* 2019;18:e12583.
50. Morgan D, Grant KA, Prioleau OA, Nader SH, Kaplan JR, Nader MA. Predictors of social status in cynomolgus monkeys (*Macaca fascicularis*) after group formation. *Am J Primatol.* 2000;52:115–31.
51. Czoty PW, Gould RW, Nader MA. Relationship between social rank and cortisol and testosterone concentrations in male cynomolgus monkeys (*Macaca fascicularis*). *J Neuroendocrinol.* 2009;21:68–76.
52. Kromrey SA, Czoty PW, Nader SH, Register TC, Nader MA. Preclinical laboratory assessments of predictors of social rank in female cynomolgus monkeys. *Am J Primatol.* 2016;78:402–17.
53. Riddick NV, Czoty PW, Gage HD, Kaplan JR, Nader SH, Icenhower M, et al. Behavioral and neurobiological characteristics influencing social hierarchy formation in female cynomolgus monkeys. *Neuroscience.* 2009;158:1257–65.
54. Zheng MQ, Kim SJ, Holden D, Lin SF, Need A, Rash K, et al. An improved antagonist radiotracer for the kappa-opioid receptor: Synthesis and characterization of (11)C-LY2459989. *J Nucl Med.* 2014;55:1185–91.
55. Gunn RN, Gunn SR, Cunningham VJ. Positron emission tomography compartmental models. *J Cereb Blood Flow Metab.* 2001;21:635–52.
56. Patterson SA, Deep G, Brinkley TE. Detection of the receptor for advanced glycation endproducts in neuronally-derived exosomes in plasma. *Biochem Biophys Res Commun.* 2018;500:892–6.
57. Ramekte A, Ting H, Agarwal C, Mateen S, Somasagara R, Hussain A, et al. Exosomes secreted under hypoxia enhance invasiveness and stemness of prostate cancer cells by targeting adherens junction molecules. *Mol Carcinog.* 2015;54:554–65.
58. Chevé M, Finkel EA, Kim SJ, O'Connor DH, Brown SP. Neural activity in the mouse claustrum in a cross-modal sensory selection task. *Neuron* 2022;110:486–501.
59. Acheson A, Robinson JL, Glahn DC, Livallo WR, Fox PT. Differential activation of the anterior cingulate cortex and caudate nucleus during a gambling simulation in persons with a family history of alcoholism: studies from the Oklahoma Family Health Patterns Project. *Drug Alcohol Depend.* 2009;100:17–23.
60. Perry JL, Joseph JE, Jiang Y, Zimmerman RS, Kelly TH, Darna M, et al. Prefrontal cortex and drug abuse vulnerability: Translation to prevention and treatment interventions. *Brain Res Rev.* 2011;65:124–49.
61. Nader MA, Czoty PW, Nader SH, Morgan D. Nonhuman primate models of social behavior and cocaine abuse. *Psychopharmacol (Berl).* 2012;224:57–67.
62. Clark SD, Abi-Dargham A. The role of dynorphin and the Kappa Opioid receptor in the symptomatology of schizophrenia: A review of the evidence. *Biol Psychiatry.* 2019;86:502–11.
63. Ji MJ, Yang J, Gao ZQ, Zhang L, Liu C. The role of the Kappa opioid system in comorbid pain and psychiatric disorders: Function and implications. *Front Neurosci.* 2021;15:642493.

64. Jacobson ML, Browne CA, Lucki I. Kappa Opioid receptor antagonists as potential therapeutics for stress-related disorders. *Annu Rev Pharm Toxicol*. 2020;60:615–36.
65. Peckys D, Landwehrmeyer GB. Expression of mu, kappa, and delta opioid receptor messenger RNA in the human CNS: a 33P in situ hybridization study. *Neuroscience*. 1999;88:1093–135.
66. Sim-Selley LJ, Daunais JB, Porrino LJ, Childers SR. Mu and kappa1 opioid-stimulated [35S]guanylyl-5'-O-(gamma-thio)-triphosphate binding in cynomolgus monkey brain. *Neuroscience*. 1999;94:651–62.
67. Goll Y, Atlan G, Citri A. Attention: The claustrum. *Trends Neurosci*. 2015;38:486–95.
68. Jackson J, Smith JB, Lee AK. The anatomy and physiology of claustrum-cortex interactions. *Annu Rev Neurosci*. 2020;43:231–47.
69. Nikolenko VN, Rizaeva NA, Beeraka NM, Oganessian MV, Kudryashova VA, Dubovets AA, et al. The mystery of claustral neural circuits and recent updates on its role in neurodegenerative pathology. *Behav Brain Funct*. 2021;17:8.
70. Liu J, Wu R, Johnson B, Vu J, Bass C, Li JX. The claustrum-prefrontal cortex pathway regulates impulsive-like behavior. *J Neurosci*. 2019;39:10071–80.
71. Van Horn JD. What is old is new again: Investigating and analyzing the mysteries of the claustrum. *Neuroinformatics*. 2019;17:1–3.
72. Smith JB, Lee AK, Jackson J. The claustrum. *Curr Biol*. 2020;30:R1401–R1406.
73. Sahara T, Nakayama K, Inoue O, Fukuda H, Shimizu M, Mori A, et al. D1 dopamine receptor binding in mood disorders measured by positron emission tomography. *Psychopharmacol (Berl)*. 1992;106:14–8.
74. Craig AD. How do you feel? Interoception: the sense of the physiological condition of the body. *Nat Rev Neurosci*. 2002;3:655–66.
75. Paulus MP, Stein MB. An insular view of anxiety. *Biol Psychiatry*. 2006;60:383–7.
76. Uddin LQ, Nomi JS, Hébert-Seropian B, Ghaziri J, Boucher O. Structure and function of the human insula. *J Clin Neurophysiol*. 2017;34:300–6.
77. Ibrahim C, Rubin-Kahana DS, Pushparaj A, Musiol M, Blumberger DM, Daskalakis ZJ, et al. The Insula: A brain stimulation target for the treatment of addiction. *Front Pharm*. 2019;10:720.
78. Craig AD. Interoception: The sense of the physiological condition of the body. *Curr Opin Neurobiol*. 2003;13:500–5.
79. Paulus MP, Tapert SF, Schulteis G. The role of interoception and alliesthesia in addiction. *Pharm Biochem Behav*. 2009;94:1–7.
80. Volkow ND, Michaelides M, Baler R. The neuroscience of drug reward and addiction. *Physiol Rev*. 2019;99:2115–40.
81. Droutman V, Bechara A, Read SJ. Roles of the different sub-regions of the insular cortex in various phases of the decision-making process. *Front Behav Neurosci*. 2015;9:309.
82. Naqvi NH, Rudrauf D, Damasio H, Bechara A. Damage to the insula disrupts addiction to cigarette smoking. *Science*. 2007;315:531–4.
83. Suñer-Soler R, Grau A, Gras ME, Font-Mayolas S, Silva Y, Dávalos A, et al. Smoking cessation 1 year poststroke and damage to the insular cortex. *Stroke*. 2012;43:131–6.
84. Abdolahi A, Williams GC, Benesch CG, Wang HZ, Spitzer EM, Scott BE, et al. Smoking cessation behaviors three months following acute insular damage from stroke. *Addict Behav*. 2015;51:24–30.
85. Abdolahi A, Williams GC, Benesch CG, Wang HZ, Spitzer EM, Scott BE, et al. Damage to the insula leads to decreased nicotine withdrawal during abstinence. *Addiction*. 2015;110:1994–2003.
86. Abdolahi A, Williams GC, Benesch CG, Wang HZ, Spitzer EM, Scott BE, et al. Immediate and sustained decrease in smoking urges after acute insular cortex damage. *Nicotine Tob Res*. 2017;19:756–62.
87. Moran-Santa Maria MM, Hartwell KJ, Hanlon CA, Canterberry M, Lematty T, Owens M, et al. Right anterior insula connectivity is important for cue-induced craving in nicotine-dependent smokers. *Addict Biol*. 2015;20:407–14.
88. Rotge JY, Cocker PJ, Daniel ML, Belin-Rauscent A, Everitt BJ, Belin D. Bidirectional regulation over the development and expression of loss of control over cocaine intake by the anterior insula. *Psychopharmacol (Berl)*. 2017;234:1623–31.
89. Schacht JP, Anton RF, Myrick H. Functional neuroimaging studies of alcohol cue reactivity: a quantitative meta-analysis and systematic review. *Addict Biol*. 2013;18:121–33.
90. Janes AC, Pizzagalli DA, Richardt S, deB Frederick B, Chuzi S, Pachas G, et al. Brain reactivity to smoking cues prior to smoking cessation predicts ability to maintain tobacco abstinence. *Biol Psychiatry*. 2010;67:722–9.
91. Dinur-Klein L, Dannon P, Hadar A, Rosenberg O, Roth Y, Kotler M, et al. Smoking cessation induced by deep repetitive transcranial magnetic stimulation of the prefrontal and insular cortices: a prospective, randomized controlled trial. *Biol Psychiatry*. 2014;76:742–9.
92. Sutherland MT, Stein EA. Functional neurocircuits and neuroimaging biomarkers of tobacco use disorder. *Trends Mol Med*. 2018;24:129–43.
93. Zangen A, Moshe H, Martinez D, Barnea-Ygael N, Vapnik T, Bystritsky A, et al. Repetitive transcranial magnetic stimulation for smoking cessation: A pivotal multicenter double-blind randomized controlled trial. *World Psychiatry*. 2021;20:397–404.
94. Vijay A, Wang S, Worhunsky P, Zheng MQ, Nabulsi N, Ropchan J, et al. PET imaging reveals sex differences in kappa opioid receptor availability in humans, in vivo. *Am J Nucl Med Mol Imaging*. 2016;6:205–14.
95. Staley JK, Rothman RB, Rice KC, Partilla J, Mash DC. Kappa2 opioid receptors in limbic areas of the human brain are upregulated by cocaine in fatal overdose victims. *J Neurosci*. 1997;17:8225–33.
96. Hurd YL, Herkenham M. Molecular alterations in the neostriatum of human cocaine addicts. *Synapse*. 1993;13:357–69.
97. Banks ML, Czoty PW, Negus SS. Utility of Nonhuman Primates in Substance Use Disorders Research. *Ilar J*. 2017;58:202–15.
98. Banks ML, Negus SS. Insights from Preclinical Choice Models on Treating Drug Addiction. *Trends Pharm Sci*. 2017;38:181–94.
99. Negus SS, Banks ML. Modulation of drug choice by extended drug access and withdrawal in rhesus monkeys: Implications for negative reinforcement as a driver of addiction and target for medications development. *Pharm Biochem Behav*. 2018;164:32–9.
100. Zamarripa CA, Naylor JE, Huskinson SL, Townsend EA, Prisinzano TE, Freeman KB. Kappa opioid agonists reduce oxycodone self-administration in male rhesus monkeys. *Psychopharmacol (Berl)*. 2020;237:1471–80.
101. Hutsell BA, Cheng K, Rice KC, Negus SS, Banks ML. Effects of the kappa opioid receptor antagonist nor-binaltorphimine (nor-BNI) on cocaine versus food choice and extended-access cocaine intake in rhesus monkeys. *Addict Biol*. 2016;21:360–73.
102. FDA. *Ketamine Hydrochloride*, D.o.H.a.H. Services, Editor. 2018, Food and Drug Administration.

## ACKNOWLEDGEMENTS

The authors thank Michael Collier, Jillian Odom, Suzy Kim and Stephanie Rideout for excellent technical assistance and Mia Allen for comments on an earlier version of this manuscript.

## AUTHOR CONTRIBUTIONS

BNJ, GD, and MAN designed the experiment. BNJ, KSS, SHN, SL, BAR, and YH conducted PET imaging studies and analyses. BNJ, AK, YS, SS, BAR, and GD conducted exosome studies and analyses. BNJ, AK, SHN, BAR, GD, and MAN wrote the manuscript. All authors reviewed the manuscript.

## FUNDING

This research was supported by grants R01 DA017763 (MAN), R01 DA049267 (GD and MAN), F31 DA053776 (BNJ), and T31 DA041349 (SR Jones, PI) from the National Institute on Drug Abuse.

## COMPETING INTERESTS

The authors declare no competing interests.

## ADDITIONAL INFORMATION

**Supplementary information** The online version contains supplementary material available at <https://doi.org/10.1038/s41386-022-01444-9>.

**Correspondence** and requests for materials should be addressed to Gagan Deep or Michael A. Nader.

**Reprints and permission information** is available at <http://www.nature.com/reprints>

**Publisher's note** Springer Nature remains neutral with regard to jurisdictional claims in published maps and institutional affiliations.

Springer Nature or its licensor holds exclusive rights to this article under a publishing agreement with the author(s) or other rightsholder(s); author self-archiving of the accepted manuscript version of this article is solely governed by the terms of such publishing agreement and applicable law.